Syntheses and Magnetic Properties of Ruthenium(II,III) Pivalate Dimers Axially Coordinated by Nitronyl Nitroxide Radicals $[Ru_2(O_2CCMe_3)_4(L)_2]BF_4$ and $[\{Ru_2(O_2CCMe_3)_4(L)_2\}\{Ru_2(O_2CCMe_3)_4(H_2O)_2\}]_n(BF_4)_{2n}$, L = 2,4,4,5,5-Pentamethyl-4,5-dihydro-1*H*-imidazol-1-oxyl-3-*N*-oxide and 2-Ethyl-4,4,5,5-tetramethyl-4,5-dihydro-1*H*-imidazol-1-oxyl-3-*N*-oxide

Yasuyoshi Sayama,† Makoto Handa,* Masahiro Mikuriya,*,† Ichiro Hiromitsu, and Kuninobu Kasuga

Department of Material Science, Interdisciplinary Faculty of Science and Engineering, Shimane University, 1060 Nishikawatsu, Matsue 690-8504

†Department of Chemistry, School of Science and Technology, Kwansei Gakuin University, 2-1 Gakuen, Sanda 669-1337

(Received September 13, 2002)

The reaction of $[Ru_2^{II,III}(O_2CCMe_3)_4]BF_4$ with nitronyl nitroxide radicals (2,4,4,5,5-pentamethyl-4,5-dihydro-1*H*-imidazol-1-oxyl-3-*N*-oxide (nitme) and 2-ethyl-4,4,5,5-tetramethyl-4,5-dihydro-1*H*-imidazol-1-oxyl-3-*N*-oxide (nitet)) in CH_2Cl_2/hexane gave dimer and chain complexes $[Ru_2(O_2CCMe_3)_4(L)_2]BF_4$ and $[\{Ru_2(O_2CCMe_3)_4(L)_2\}\{Ru_2(O_2CCMe_3)_4(H_2O)_2\}]_n(BF_4)_{2n}$ (L = nitme and nitet). The latter complexes have a chain structure formed by hydrogen bonds between the axial radical ligands and the water molecules. It was shown that the antiferromagnetic interaction between the coordinated radicals through the Ru–Ru bond as well as the ferromagnetic interaction between the radical and the Ru(II,III) dimeric core are operative for all of the complexes. Both of the magnetic interactions were concluded to result from their axial Ru–O_{ax}–N bond angles being close to 120°. The hydrogen bonds were not found to be magnetically important in the chain complexes.

In the metal carboxylate dimers ($[M_2(O_2CR)_4]^{m+}$, $m = 0$–2) with a lantern-like structure, the ruthenium(II,II or II,III) dimers are quite unique because they are paramagnetic with two or three unpaired electrons accommodated in their degenerated π^* and δ^* orbitals based on the metal–metal bond ($\sigma^2\pi^4\delta^2(\pi^*\delta^*)^4$ (for Ru(II,II)) and $\sigma^2\pi^4\delta^2(\pi^*\delta^*)^3$ (for Ru(II,III)) electronic structures).[1,2] Many efforts have been made to use dimers as building blocks in combination with bridging ligands to produce new magnetic or conductive materials.[3–5] In order to obtain such compounds, we chose nitroxide radicals as the bridging ligands.[5] These radicals have been known to be magnetically talented ligands, and are widely utilized to prepare metal complexes with them,[6] since ferrimagnetic chain compounds with nitronyl nitroxide radical ligands were presented by Gatteschi's and Rey's groups.[7] Nitroxide complexes of metal carboxylate dimers have recently been prepared and investigated concerning their magnetic properties.[5,8–10] We prepared a chain complex of ruthenium(II,III) pivalate dimer, $[Ru_2(O_2CCMe_3)_4(nitph)]_n(BF_4)_n$ (**1**), nitph = 2-phenyl-4,4,5,5-tetramethyl-4,5-dihydro-1*H*-imidazol-1-oxyl-3-*N*-oxide, in the hope that it would exhibit a ferrimagnetic behavior due to its alternated arrangement of the Ru(II,III) dimer ($S = 3/2$) and the nitroxide radical ($S = 1/2$) by an axial coordination of the radical to the Ru(II,III) dimer core. However, such a behavior has not been observed for complex **1**; the magnetic moment decreased steadily with lowering the temperature, which was accounted for in terms of an unsuitable axial Ru–O_{ax}–N bond angle for giving the ferrimagnetic behavior.[5c] Based on this result, we carried on the syntheses of ruthenium(II,III) complexes using other nitroxide radicals with the expectation that the Ru–O_{ax}–N bond angle could be favorably changed by replacing the phenyl group.

In this study, we employed 2,4,4,5,5-pentamethyl-4,5-dihydro-1*H*-imidazol-1-oxyl-3-*N*-oxide (nitme) and 2-ethyl-4,4,5,5-tetramethyl-4,5-dihydro-1*H*-imidazol-1-oxyl-3-*N*-oxide (nitet) as the radical ligands. In addition to bis(nitroxide) complexes of the Ru(II,III) dimer, $[Ru_2(O_2CCMe_3)_4(L)_2]BF_4$ (**2** (L = nitme) and **3** (L = nitet)), we isolated complexes with the stoichiometry of Ru(II,III):L:BF_4^-=1:1:1. Although the desired chain structure with an alternated Ru(II,III)-nitroxide arrangement was not formed in this combination, novel chain complexes, $[\{Ru_2(O_2CCMe_3)_4(L)_2\}\{Ru_2(O_2CCMe_3)_4(H_2O)_2\}]_n(BF_4)_{2n}\cdot 2nCH_2Cl_2$ (**4** (L = nitme) and **5** (L = nitet)), in which hydrogen bonds between axial nitroxide ligands and water molecules work as junctions to connect the Ru(II,III) dimers and the radicals to give chain structures, were obtained. Here, we report on the structures and magnetic properties of discrete dimer and chain complexes of ruthenium(II,III) pivalate with nitroxide radicals at the axial positions. Two different magnetic interactions (one is between the Ru(II,III) dimeric core and the coordinated radical, and the other is between the radicals through the Ru–Ru bond) are also discussed regarding the axial Ru–N_{ax}–O (nitroxide) bond angles. A preliminary report has been published for complex **4**.[5e]

Experimental

Preparation. The tetrafluoroborate salt $[Ru_2(O_2CCMe_3)_4(H_2O)_2]BF_4$ was prepared according to a method described in the literature.[11] The nitronyl nitroxide radicals nitme and nitet were obtained according to a method described in the literature.[12]

$[Ru_2(O_2CCMe_3)_4(nitme)_2]BF_4 \cdot 2CH_2Cl_2$ (2). A 20 mg (0.027 mmol) portion of $[Ru_2(O_2CCMe_3)_4(H_2O)_2]BF_4$ was put into a Schlenk tube and heated at 80 °C under a vacuum for thirty minutes in order to remove the axial water molecules, during which treatment the tetrafluoroborate salt turned yellowish brown from orange. A CH_2Cl_2 solution (4 cm^3) of nitme (11 mg (0.064 mmol)) was then added into the tube and stirred with the water-removed tetrafluoroborate salt under argon. Onto the reacted solution was slowly added hexane (15 cm^3); the resulting solution was allowed to stand for several days at room temperature to deposit purple crystals, which were collected by filtration and washed with hexane. The yield was 24 mg (73% based on $[Ru_2(O_2CCMe_3)_4(H_2O)_2]BF_4$). Anal. Found: C, 37.63; H, 5.84; N, 4.59%. Calcd for $C_{38}H_{70}BCl_4F_4N_4O_{12}Ru_2$: C, 37.85; H, 5.85; N, 4.65%. IR (in KBr) ν(NO) 1372, ν(COO) 1486, 1455, 1422, $\nu(BF_4^-)$ 1058 cm^{-1}. Diffuse reflectance spectrum: λ_{max} 315, 539, 641, 1066(br) nm.

$[Ru_2(O_2CCMe_3)_4(nitet)_2]BF_4 \cdot 2CH_2Cl_2$ (3). This compound was obtained as purple crystals by the reaction of $[Ru_2(O_2CCMe_3)_4(H_2O)_2]BF_4$ (20 mg, 0.027 mmol) with nitet (12.3 mg, 0.066 mmol) in CH_2Cl_2/hexane using the same method as that of **2**. The yield was 22 mg (64% based on $[Ru_2(O_2CCMe_3)_4(H_2O)_2]BF_4$). Anal. Found: C, 39.06; H, 6.21; N, 4.30%. Calcd for $C_{40}H_{74}BCl_4F_4N_4O_{12}Ru_2$: C, 38.93; H, 6.04; N, 4.54%. IR (in KBr) ν(NO) 1360, ν(COO) 1487, 1456, 1423, $\nu(BF_4^-)$ 1056 cm^{-1}. Diffuse reflectance spectrum: λ_{max} 312, 539, 626, 1072 (br) nm.

$[\{Ru_2(O_2CCMe_3)_4(nitme)_2\}\{Ru_2(O_2CCMe_3)_4(H_2O)_2\}]_n(BF_4)_{2n} \cdot 2nCH_2Cl_2$ (4). A 20 mg (0.027 mmol) portion of $[Ru_2(O_2CCMe_3)_4(H_2O)_2]BF_4$ was put into a Schlenk tube and heated at 80 °C under a vacuum for thirty minutes in order to remove the axial water molecules. The CH_2Cl_2 solution (4 cm^3) of nitme (4.8 mg (0.028 mmol)) was then added into the tube and stirred with the water-removed tetrafluoroborate salt under argon. Onto the reacted solution was slowly added hexane (15 cm^3); the resulting solution was allowed to stand for several days at room temperature to deposit purple crystals, which were collected by filtration and washed with hexane. The yield was 16 mg (62% based on $[Ru_2(O_2CCMe_3)_4(H_2O)_2]BF_4$). Anal. Found: C, 36.27; H, 5.91; N, 2.93%. Calcd for $C_{58}H_{110}B_2Cl_4F_8N_4O_{22}Ru_4$: C, 35.99; H, 5.73; N, 2.89%. IR (in KBr) ν(NO) 1375, ν(COO) 1486, 1454, 1423, $\nu(BF_4^-)$ 1080 cm^{-1}. Diffuse reflectance spectrum: λ_{max} 319, 410(sh), 536, 643(sh), 1046(br) nm.

$[\{Ru_2(O_2CCMe_3)_4(nitet)_2\}\{Ru_2(O_2CCMe_3)_4(H_2O)_2\}]_n(BF_4)_{2n} \cdot 2nCH_2Cl_2$ (5). This compound was obtained as purple crystals by the reaction of $[Ru_2(O_2CCMe_3)_4(H_2O)_2]BF_4$ (20 mg, 0.027 mmol) with nitet (5.4 mg, 0.029 mmol) in CH_2Cl_2/hexane using the same method as that of **4**. The yield was 19 mg (70% based on $[Ru_2(O_2CCMe_3)_4(H_2O)_2]BF_4$). Anal. Found: C, 36.90; H, 5.97; N, 2.77%. Calcd for $C_{60}H_{114}B_2Cl_4F_8N_4O_{22}Ru_4$: C, 36.70; H, 5.85; N, 2.85%. IR (in KBr) ν(NO) 1367, ν(COO) 1486, 1454, 1423, $\nu(BF_4^-)$ 1076 cm^{-1}. Diffuse reflectance spectrum: λ_{max} 320, 535, 644, 1065(br) nm.

Measurements. Elemental analyses for carbon, hydrogen, and nitrogen were carried out using a Perkin-Elmer Series II, CHN/O Analyzer. Infrared spectra (KBr pellets) and electronic spectra were measured with JASCO IR-700 and Shimadzu UV-3100 spectrometers, respectively. The magnetic susceptibilities were measured over the 2–300 K temperature range on a Quantum Design MPMS-5S SQUID susceptometer operating under a magnetic field of 0.5 T. The susceptibilities were corrected for the diamagnetism of the constituent atoms using Pascal's constant.[13] The effective magnetic moments were calculated using the equation $\mu_{eff} = 2.828\sqrt{\chi_M T}$, where χ_M is the magnetic susceptibility per $Ru_2^{II,III}$–(nitroxide)$_2$ unit for **2** and **3** and per $[Ru_2^{II,III}$–(nitroxide)$]_2$ for **4** and **5**. The ESR measurement was performed on a home-made *K*-band (23 GHz) apparatus employing a microwave power of 20 mW and with a magnetic field modulation frequency of 100 kHz and an intensity of 0.5 G (1 G = 1×10^{-4} T).

Table 1. Crystal Data and Data Collection Details of **2**, **4**, and **5**

Complex	**2**	**4**	**5**
Formula	$C_{38}H_{70}BCl_4F_4N_4O_{12}Ru_2$	$C_{58}H_{110}B_2Cl_4F_8N_4O_{22}Ru_4$	$C_{60}H_{114}B_2Cl_4F_8N_4O_{22}Ru_4$
F.W.	1205.95	1935.63	1963.68
Crystal system	orthorhombic	monoclinic	monoclinic
Space group	*Pbcn*	*C*2/*c*	*C*2/*c*
a/Å	18.370(1)	46.695(14)	46.705(19)
b/Å	16.464(1)	10.404(2)	10.413(1)
c/Å	18.191(1)	18.273 (2)	18.940(5)
β/°		105.03(1)	105.71(1)
V/Å^3	5502(1)	8574(4)	8867(4)
Z	4	4	4
D_c/g cm^{-3}	1.46	1.50	1.47
D_m/g cm^{-3}	1.46	1.49	1.47
Crystal size/mm	0.48 × 0.45 × 0.15	0.42 × 0.40 × 0.10	0.38 × 0.30 × 0.18
μ(Mo Kα)/cm^{-1}	8.00	8.82	8.54
2θ range/°	1–49	1–48	1–48
No. of reflections measured	5082	7114	7355
No. of unique reflections with $I > 3\sigma(I)$	2870	3722	3041
Final no. of variables	299	485	469
R	0.045	0.056	0.055
R_w	0.052	0.064	0.062

Table 2. Selected Bond Distances (Å) and Angles (°) of **2**, **4**, and **5** with Their Estimated Standard Deviations in Parentheses

2[a]			
Ru–Ru′	2.272(1)	Ru–O5	2.239(4)
Ru–O1	2.019(4)	N1–O5	1.305(7)
Ru–O2	2.018(4)	N2–O6	1.269(8)
Ru–O3	2.028(4)	Ru′–Ru–O5	177.3(1)
Ru–O4	2.019(4)	Ru–O5–N1	123.7(4)
4[b]			
Ru1–Ru1′	2.275(1)	Ru2–O7	2.024(8)
Ru1–O1	2.015(7)	Ru2–O8	2.037(8)
Ru1–O2	2.021(7)	Ru2–O11	2.248(7)
Ru1–O3	2.013(7)	N1–O9	1.31(1)
Ru1–O4	2.031(7)	N2–O10	1.28(1)
Ru1–O9	2.269(8)	Ru1′–Ru1–O9	177.7(2)
Ru2–Ru2″	2.262(1)	Ru2″–Ru2–O11	174.3(2)
Ru2–O5	2.014(8)	Ru1–O9–N1	121.5(6)
Ru2–O6	2.024(8)		
5[c]			
Ru1–Ru1′	2.273(2)	Ru2–O6	2.022(9)
Ru1–O1	2.016(8)	Ru2–O7	2.011(9)
Ru1–O2	2.026(8)	Ru2–O8	2.014(9)
Ru1–O3	2.014(8)	Ru2–O11	2.278(8)
Ru1–O4	2.017(8)	N1–O9	1.31(1)
Ru1–O9	2.270(9)	N2–O10	1.28(1)
Ru2–Ru2″	2.256(1)	Ru1′–Ru1–O9	176.6(2)
Ru2–O5	2.003(9)	Ru2″–Ru2–O11	175.7(3)
Ru2–O6	2.022(9)	Ru1–O9–N1	122.5(7)

a) Prime refers to the equivalent position $(-x, y, 1/2 - z)$. b) Prime refers to the equivalent position $(1/2 - x, 1/2 - y, 1 - z)$. Double prime refers to the equivalent position $(1 - x, -y, -z)$. c) Prime refers to the equivalent position $(3/2 - x, 1/2 - y, 1 - z)$. Prime refers to the equivalent position $(-x, 1 - y, -z)$.

X-ray Crystal Structure Analysis. Diffraction data were collected on an Enraf–Nonius CAD4 diffractometer using graphite-monochromated Mo Kα radiation at 25 ± 1 °C. Crystal data and details concerning the data collection are given in Table 1. The lattice constants were determined by a least-squares refinement based on 25 reflections with $20 \leq 2\theta \leq 30°$. The intensity data were corrected for Lorentz-polarization effects. The structures were solved by direct methods. Refinements were carried out by full-matrix least-squares methods. Non-hydrogen atoms were refined with anisotropic thermal parameters. There are disorders at the carbon atoms of *t*-butyl groups for **4**; hence, their positions were divided into two positions (C4a, C5a, C8a, C9a, and C10a are one of each pair of them in Fig. 2). Hydrogen atoms were fixed at their calculated positions. A weighting scheme, $w = 1/[\sigma^2(|F_o|) + (0.02|F_o|)^2 + 1.0]$, was employed. The final discrepancy factors, $R = \Sigma \parallel F_o| - |F_c \parallel / \Sigma|F_o|$ and $R_w = [\Sigma w(|F_o| - |F_c|)^2 / \Sigma w|F_o|^2]^{1/2}$, are listed in Table 1. All of the calculations were carried out on a micro VAX station 4000 90A computer using a MolEN program package.[14] Selected bond distances and angles of **2**, **4**, and **5** are listed in Table 2. Crystallographic data have been deposited at the CCDC, 12 Union Road, Cambridge CB2 1EZ, UK; copies can be obtained on request, free of charge, by quoting the publication citation and deposition numbers (CCDC 202139–202141).

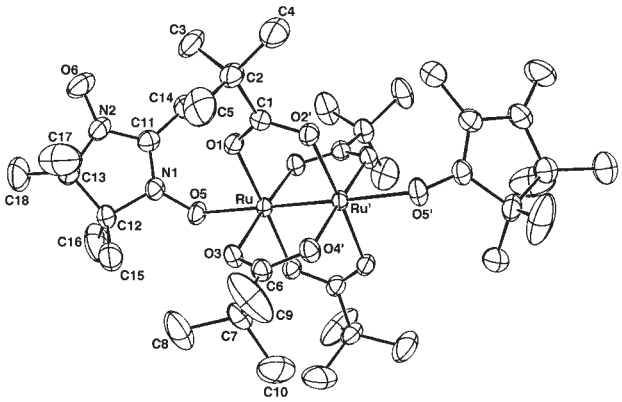

Fig. 1. Perspective view of $[Ru_2(O_2CCMe_3)_4(nitme)_2]$-$BF_4 \cdot 2CH_2Cl_2$ (**2**). The CH_2Cl_2 molecules and BF_4 ions are omitted for clarity. Primes refer to the equivalent positions $(-x, y, 1/2 - z)$.

Results and Discussion

Syntheses. The dimer complexes $[Ru_2(O_2CCMe_3)_4(L)_2]$-$BF_4 \cdot 2CH_2Cl_2$ (**2** and **3**) or the chain complexes $[\{Ru_2$-$(O_2CCMe_3)_4(L)_2\}\{Ru_2(O_2CCMe_3)_4(H_2O)_2\}]_n(BF_4)_{2n} \cdot 2nCH_2$-$Cl_2$ (**4** and **5**), L = nitme and nitet, were formed depending on the Ru(II,III)–radical mole ratio employed for the reaction. The excess (at least twice in mole amount) of the radical ligands to the ruthenium(II,III) pivalate dimer was needed to exclusively obtain dimer complexes **2** and **3**. In a 1:1 reaction of the Ru(II,III) dimer and the ligands, chain complexes **4** and **5** were predominantly isolated. Our efforts to obtain single crystals for the chain complexes of the radicals without water molecules were unsuccessful.

Structural Descriptions. $[Ru_2(O_2CCMe_3)_4(nitme)_2]$-$BF_4 \cdot 2CH_2Cl_2$ (2). The crystal structure of **2** is depicted in Fig. 1. The lantern-like framework made up by two ruthenium ions and four pivalate ions is preserved in **2**, having nitroxide (nitme) molecules at the axial positions. The inversion center is located at the center of the dimer core. The Ru–Ru′ distance (2.272(1) Å) is in the range of those for $[Ru_2(O_2CR)_4]^+$ compounds (2.24–2.30 Å).[1] The axial Ru–O5 distance is 2.239(4) Å, nearly the same as that of the corresponding distances (2.236(8) and 2.264(8) Å) for **1**.[5c] The N–O bond lengths, 1.305(7) (for N1–O5) and 1.269(8) (for N2–O6), confirm that the ligand nitme exists as a free radical.[15,16] One (N2–O6) of the two N–O groups of the nitme molecule does not participate in the coordination, which could be the reason for the shorter N–O bond length (1.269(8) Å).

$[\{Ru_2(O_2CCMe_3)_4(nitme)_2\}\{Ru_2(O_2CCMe_3)_4(H_2O)_2\}]_n$-$(BF_4)_{2n} \cdot 2nCH_2Cl_2$ (4). The crystal consists of two kinds of Ru(II,III) dimer units, $[Ru_2(O_2CCMe_3)_4(nitme)_2]^+$ and $[Ru_2$-$(O_2CCMe_3)_4(H_2O)_2]^+$. The crystallographic inversion centers are located at the centers of both of the dimer cores. The structure of the dimer unit, $[Ru_2(O_2CCMe_3)_4(nitme)_2]^+$, is shown in Fig. 2. The apical sites of the one Ru(II,III) core are occupied by the nitme molecules with a distance of Ru1–O9 = 2.269(8) Å. One of the two NO groups of nitme remains uncoordinated, as in the case of **2**; the N–O bond length of the uncoordinated one is 1.28(1) Å (for N2–O10), while that of the coordinated one is 1.31 Å (for N1–

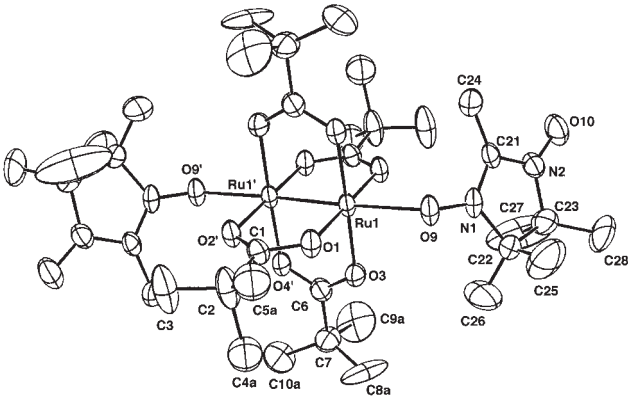

Fig. 2. Perspective view of $[Ru_2(O_2CCMe_3)_4(nitme)_2]^+$ dimer unit in $[\{Ru_2(O_2CCMe_3)_4(nitme)_2\}\{Ru_2(O_2CCMe_3)_4(H_2O)_2\}]_n(BF_4)_{2n}\cdot 2nCH_2Cl_2$ (**4**). Primes refer to the equivalent positions $(1/2 - x, 1/2 - y, 1 - z)$.

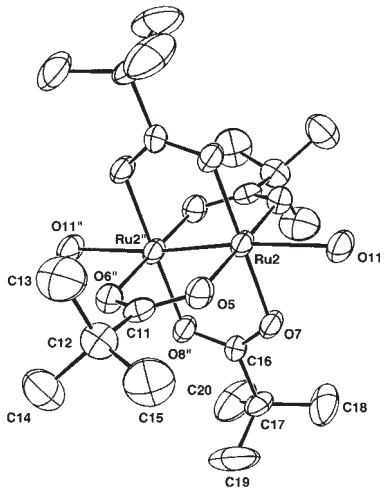

Fig. 3. Perspective view of $[Ru_2(O_2CCMe_3)_4(H_2O)_2]^+$ dimer unit in $[\{Ru_2(O_2CCMe_3)_4(nitme)_2\}\{Ru_2(O_2CCMe_3)_4(H_2O)_2\}]_n(BF_4)_{2n}\cdot 2nCH_2Cl_2$ (**4**). Double primes refer to the equivalent positions $(1 - x, -y, -z)$.

O9). In Fig. 3, the structure of the dimer unit, $[Ru_2(O_2CCMe_3)_4(H_2O)_2]^+$, is depicted. The water molecules are axially coordinated to the dimer core with a distance of Ru2–O11 = 2.248(7) Å. The Ru–Ru distances are 2.275(1) (for the nitme coordinated dimer unit (Ru1–Ru1′)) and 2.262(1) Å (for the water-coordinated dimer unit (Ru2–Ru2″)), which are in the range for those of Ru(II,III) carboxylates.[1] The dimer units, $[Ru_2(O_2CCMe_3)_4(nitme)_2]^+$ and $[Ru_2(O_2CCMe_3)_4(H_2O)_2]^+$, are not discrete, but connected by using a hydrogen bond between the uncoordinated NO group of nitme and the coordinated water of the neighboring dimer units (O10···O11 = 2.81(1) Å), forming a novel chain structure with an alternated arrangement of the two kinds of dimer units. A similar hydrogen bond has been reported for a rhodium(II) carboxylate dimer with a nitroxide radial $[Rh_2(O_2CCCF_3)_4(H_2O)_2]\cdot 2$DTBN (DTBN = di-*tert*-butyl nitroxide), in which the corresponding O···O distances are 2.799(3) and 2.776(3) Å.[17] In **4**, the coordinated water oxygen is further hydrogen-bonded to the counter ion BF_4^- with an O11···F1 (BF_4^-) distance of 2.62(2) Å, as shown in Fig. 4, the bonding mode also being seen for **5** (vide infra). A "dimer-of-dimers"

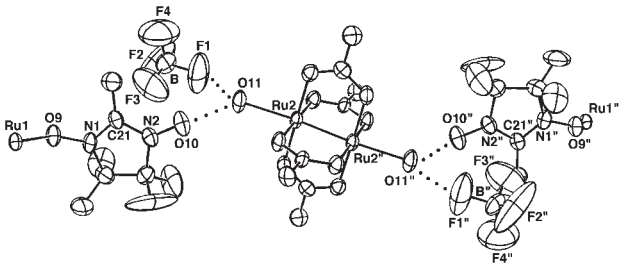

Fig. 4. View of hydrogen bonds in $[\{Ru_2(O_2CCMe_3)_4(nitme)_2\}\{Ru_2(O_2CCMe_3)_4(H_2O)_2\}]_n(BF_4)_{2n}\cdot 2nCH_2Cl_2$ (**4**). The methyl groups on the pivalate ions and CH_2Cl_2 molecules are omitted for clarity. Primes and double primes refer to the equivalent positions $(1/2 - x, 1/2 - y, 1 - z)$ and $(1 - x, -y, -z)$, respectively.

complex, $[Ru_2(O_2CCMe_3)_4(nitph)(H_2O)(\mu\text{-}BF_4)]_2$ (**6**), has BF_4^- ions intervening between the Ru(II,III) dimer units with the hydrogen bonds having distances of O···F = 2.71(1) and 2.74(1) Å.[5h] The presence of two different Ru(II,III) units coordinated by two water molecules and two nitroxide N–O groups in the crystal has been presented for a nitroxide ruthenium(II,III) complex, $[Ru_2(O_2CCMe_3)_4(tempo)_2][Ru_2(O_2CCMe_3)_4(H_2O)_2](BF_4)_2$ (**7**), tempo = 2,2,6,6-tetramethylpiperidine-1-oxyl, in which the Ru(II,III) dimer units are isolated because tempo has only one NO group within the tempo molecule.[5a]

$[\{Ru_2(O_2CCMe_3)_4(nitet)_2\}\{Ru_2(O_2CCMe_3)_4(H_2O)_2\}]_n$-$(BF_4)_{2n}\cdot 2nCH_2Cl_2$ (5). The crystal structure of **5** is shown in Fig. 5. The chain structure is made up in the same way as **4**, using the hydrogen bond of the uncoordinated NO group of nitet to the coordinated water oxygen (O10···O11 = 2.78(1) Å). The oxygen atom O11 is further hydrogen-bonded to one of the fluorine atoms of BF_4^- (O11···F1 = 2.65(2) Å), similarly to **4**. The crystallographic inversion centers exist at the centers of the Ru(II,III) dimers. The Ru–Ru distances are 2.273(2) (for the nitet-coordinated dimer unit (Ru1–Ru1′) and 2.256(1) Å (for the water-coordinated dimer unit (Ru2–Ru2″)), which are in the range for those of ruthenium(II,III) carboxylates.[1] The Ru–O_{ax} distances at the axial positions are 2.270(9) (for the nitet-coordinated dimer unit (Ru1–O9)) and 2.278(8) Å (for the water-coordinated dimer unit (Ru2–O11)). The N–O bond lengths of nitet are 1.31(1) Å (for the coordinated one (N1–O9)) and 1.28(1) Å (for the uncoordinated one (N2–O10)). These Ru–Ru, Ru–O_{ax}, and N–O distances are comparable to those for **4**.

Magnetic Properties. Dimer Complexes of Ruthenium(II,III) Pivalate and Nitroxide Radical (2 and 3). The temperature dependencies of the magnetic susceptibilities and the effective magnetic moments for **2** and **3** are shown in Figs. 6 and 7. Both of the complexes show magnetic moments (5.12 B.M. for **2** and 5.11 B.M. for **3**) with values higher than that (4.58 B.M.) where three spin centers (one $S = 3/2$ (for Ru(II,III) dimer) and two $S = 1/2$ (for radical)) are magnetically independent. The moments are nearly constant in the temperature range of 100–300 K, though a maximum (5.19 B.M.) appears at 125 K for **2**. The moments then begin to decrease gradually with lowering the temperature below 100 K, and reach values (3.71 (for **2**) and 3.12 B.M. (for **3**) at 2 K) close to that for the parent dimer, $[Ru_2(O_2CCMe_3)_4]^+$ (3.24 B.M. at 2.5 K),[5f] being indicative of the existence of an antiferromagnetic interaction. The tempera-

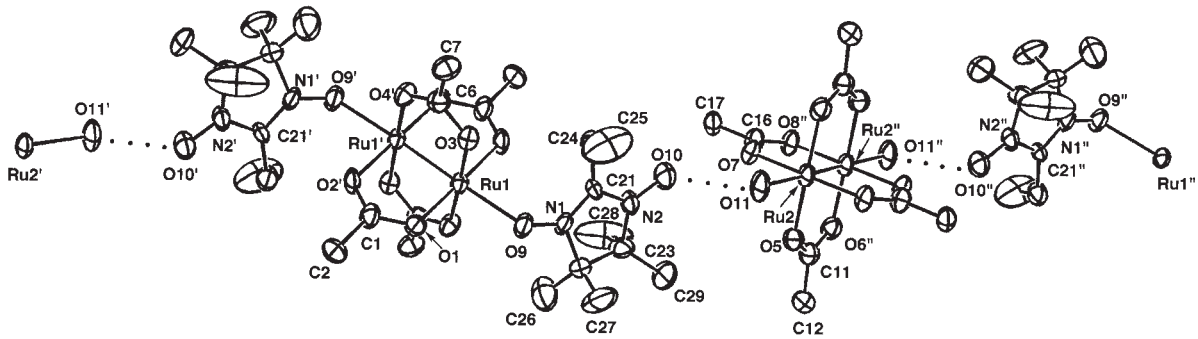

Fig. 5. Perspective view of chain structure of $[\{Ru_2(O_2CCMe_3)_4(nitet)_2\}\{Ru_2(O_2CCMe_3)_4(H_2O)_2\}]_n(BF_4)_{2n}\cdot 2nCH_2Cl_2$ (**5**). The methyl groups on the pivalate ions, CH_2Cl_2 molecules and BF_4^- ions are omitted for clarity. Primes and double primes refer to the equivalent positions $(3/2 - x, 1/2 - y, 1 - z)$ and $(-x, 1 - y, -z)$, respectively.

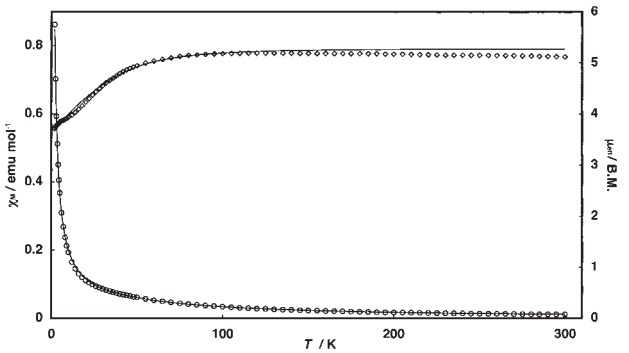

Fig. 6. Temperature dependences of magnetic susceptibility (○) and effective magnetic moment (◇) for $[Ru_2(O_2CCMe_3)_4(nitme)_2]BF_4\cdot 2CH_2Cl_2$ (**2**). The solid lines were calculated with the parameters listed in Table 3.

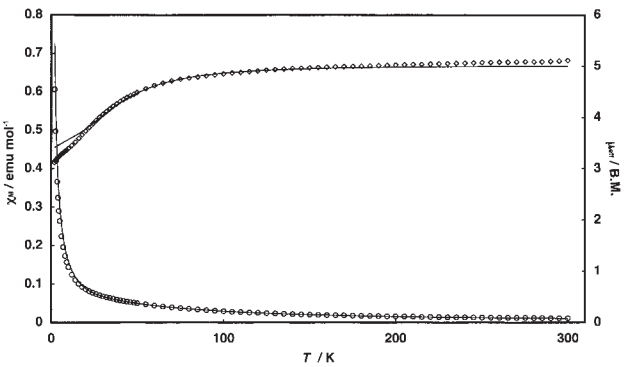

Fig. 7. Temperature dependences of magnetic susceptibility (○) and effective magnetic moment (◇) for $[Ru_2(O_2CCMe_3)_4(nitet)_2]BF_4\cdot 2CH_2Cl_2$ (**3**). The solid lines were calculated with the parameters listed in Table 3.

ture-dependent profiles of the magnetic susceptibilities and moments could be simulated based on the model illustrated in Scheme 1, where J_{M-R} is the spin-coupling constant for the interaction between the Ru(II,III) dimeric core and the radical and J_{R-R} for that between the radicals through the Ru–Ru bond. In a simulation, the g factor for the radical (g_R) was fixed at 2.00. The other parameters, g_M (the g factor for the Ru(II,III) dimeric core), D (for the zero-field splitting for the Ru(II,III) core), J_{M-R}, and J_{R-R} were estimated by fitting the theoretical magnetic susceptibilities to the experimental data. The theoretical magnetic susceptibilities

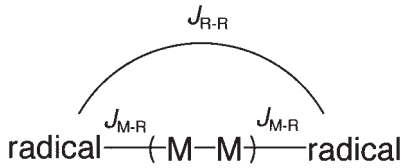

Scheme 1.

Table 3. Fitting Parameters for the Magnetic Data of **2**–**5**

Complex	**2**	**3**	**4**	**5**
g_M	2.40	2.25	2.19	2.28
g_R	2.00	2.00	2.00	2.00
J_{M-L}/cm^{-1}	5	5	20	20
J_{R-R}/cm^{-1}	−40	−40	−50	−47
D/cm^{-1}	20	40	15	22
D'/cm^{-1}			60	60
R[a)]	4.57×10^{-4}	2.56×10^{-2}	7.84×10^{-5}	7.66×10^{-5}

a) $R = \Sigma(\chi_{obsd} - \chi_{calcd})^2/\Sigma(\chi_{obsd})^2$, where χ is the magnetic susceptibility.

were numerically calculated because it was impossible to obtain an analytic formula for the theoretical magnetic susceptibilities. The same treatment on the magnetic data was performed for the bis-tempo dimer cation $[Ru_2(O_2CCMe_3)_4(tempo)_2]^+$ in $[Ru_2(O_2CCMe_3)_4(tempo)_2][Ru_2(O_2CCMe_3)_4(H_2O)_2](BF_4)_2$ (**7**).[5a] The magnetic parameters obtained by the fittings for **2** and **3** are listed in Table 3. Both of the complexes have positive J_{M-R} (5 cm^{-1}) and negative J_{R-R} (−40 cm^{-1}) values. The magnetic behaviors could not be simulated well without a positive J_{M-R} value. The bis-tempo dimer cation $[Ru_2(O_2CCMe_3)_4(tempo)_2]^+$ in **7** revealed a large minus J_{M-R} value (= −130 cm^{-1}) and a nearly zero J_{R-R} value. The difference can be explained regarding the axial Ru–O–N bond angles (∠Ru–O–N (nitme) = 123.7(4)° for **2**; ∠Ru–O–N (tempo) = 151.5(3)° for **7**) (vide infra).

Chain Complexes of Ruthenium(II,III) Pivalate and Nitroxide Radical (4 and 5). The variations in the magnetic susceptibilities and the effective magnetic moments with temperature (2–300 K) for **4** and **5** are shown in Figs. 8 and 9. The room-temperature magnetic moments of **4** and **5** are 6.63 and 6.86 B.M., respectively, which are appreciably higher than the value (6.00 B.M.) expected for the non-interacting spins, two $S = 3/2$ (for Ru(II,III) dimer) and two $S = 1/2$ (for radical). The effective magnetic moments of **4** and **5** slightly increase from room

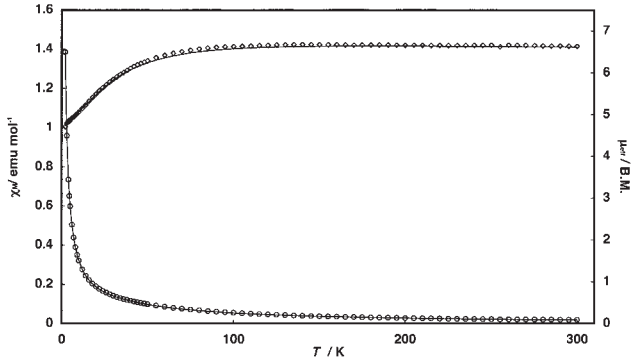

Fig. 8. Temperature dependences of magnetic susceptibility (○) and effective magnetic moment (◇) for $[\{Ru_2(O_2CCMe_3)_4(nitme)_2\}\{Ru_2(O_2CCMe_3)_4(H_2O)_2\}]_n(BF_4)_{2n}\cdot 2nCH_2Cl_2$ (**4**). The solid lines were calculated with the parameters listed in Table 3.

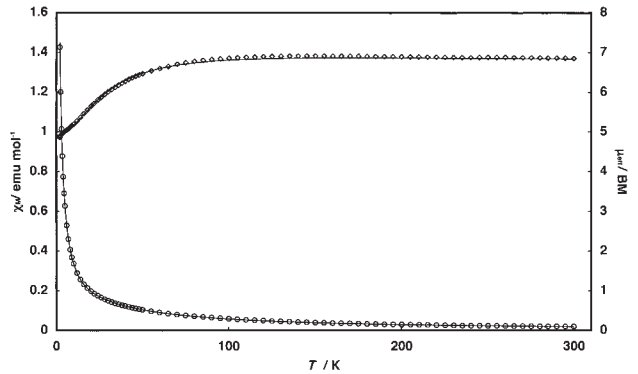

Fig. 9. Temperature dependences of magnetic susceptibility (○) and effective magnetic moment (◇) for $[\{Ru_2(O_2CCMe_3)_4(nitet)_2\}\{Ru_2(O_2CCMe_3)_4(H_2O)_2\}]_n(BF_4)_{2n}\cdot 2nCH_2Cl_2$ (**5**). The solid lines were calculated with the parameters listed in Table 3.

temperature to 140 K (6.68 B.M. for **4** and 6.91 B.M. for **5**), and are almost constant down to 100 K. Then, the moments gradually decrease with lowering the temperature, and reach values (4.71 B.M. for **4** and 4.86 B.M. for **5**) close to that (4.58 B.M. (2.5 K)) corresponding to two $[Ru_2(O_2CCMe_3)_4]^+$ parent dimers.[5f] The magnetic behaviors were simulated by assuming that the interaction through the hydrogen bonds is negligible. The magnetic susceptibilities were calculated by summing those of two magnetically independent dimer units, $[Ru_2(O_2CCMe_3)_4(L)_2]^+$ (L = nitme and nitet) and $[Ru_2(O_2CCMe_3)_4(H_2O)_2]^+$. The zero-field splitting (D') for $[Ru_2(O_2CCMe_3)_4(H_2O)_2]^+$ was set at 60 cm^{-1}, bearing in mind that $[Ru_2(O_2CCMe_3)_4(H_2O)_2]BF_4$ has a value of 60 cm^{-1}.[5a,f] The unit $[Ru_2(O_2CCMe_3)_4(L)_2]^+$ can be analyzed in the same way as that for **2** and **3**. The obtained parameters are listed in Table 3. It can be clearly seen that the solid lines drawn with the parameters in Table 3 well reproduce the temperature-dependent profiles of the susceptibilities and the moments of **4** and **5** (Figs. 8 and 9). The results indicate that the hydrogen bonds are not magnetically important in the present chain complexes. The negative J_{R-R} (−50 cm^{-1} for **4** and −47 cm^{-1} for **5**) and positive J_{M-R} value (20 cm^{-1} for **4** and **5**) were necessary for simulations as in the cases of **2** and **3**. The zero-field splitting parameters (D) of the present nitroxide complexes **2**–**5**

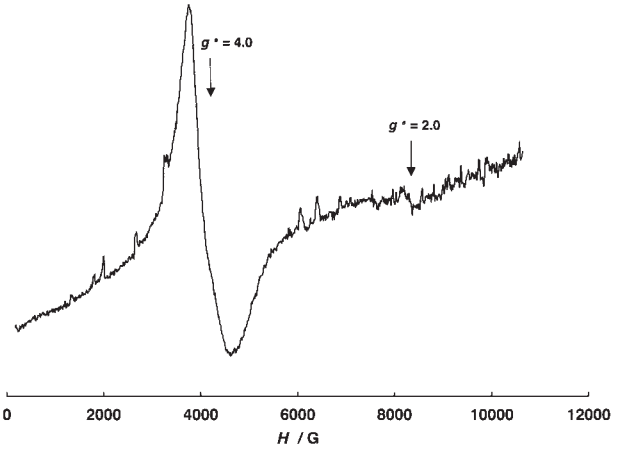

Fig. 10. ESR spectrum of $[\{Ru_2(O_2CCMe_3)_4(nitme)_2\}\{Ru_2(O_2CCMe_3)_4(H_2O)_2\}]_n(BF_4)_{2n}\cdot 2nCH_2Cl_2$ (**4**) at 30 K (*K*-band).

are 15–40 cm^{-1}, which are slightly low compared with those for the other Ru(II,III) dimers with the lantern-like structure (30–70 cm^{-1}).[3,18]

The ESR spectrum (powder at 30 K) of **4** shows strong and very weak signals at $g^e = 4.0$ and 2.0 (Fig. 10), where g^e means the effective g value.[5a] The spectral feature is different from that of **7**, which showed three signals at $g^e = 4.40$, 2.33, and 1.92.[5a] The signals at $g^e = 2.33$, and 1.92 were attributed to those for the parallel and perpendicular components in the dimer unit $[Ru_2(O_2CCMe_3)_4(tempo)_2]^+$ based on a quantum calculation in consideration of the strong antiferromagnetic interaction between the Ru(II,III) dimer core and tempo ($J_{M-R} = -130$ cm^{-1}; $J_{R-R} = 0$ cm^{-1}), giving the $S = 1/2$ ground state. The signal at $g^e = 4.40$ was assigned as the perpendicular component of $[Ru_2(O_2CCMe_3)_4(H_2O)_2]^+$ unit.[5a,18a,b] In the case of **4**, the radical–radical interaction is predominant compared with the Ru(II,III)–radical interaction ($J_{R-R} = -50$ cm^{-1}; $J_{M-R} = 20$ cm^{-1}), which gives a different spin ground state. The spins of the axial nitme radicals are considered to be washed out by the strong antiferromagnetic coupling between the radicals. The signal at $g^e = 4.0$ can be assigned as those for the perpendicular components of the $[Ru_2(O_2CCMe_3)_4]^+$ and $[Ru_2(O_2CCMe_3)_4(nitme)_2]^+$ units. The weak signal at $g^e = 2.0$ could be due to the parallel component of the Ru(II,III) dimers, the parallel signal of Ru(II,III) dimer being normally very weak,[5a,18a,b] or an impurity, such as the uncoordinated nitme radical.

Relationship between Magnetic Interaction and Axial Bond Angle. We have reported that the axial Ru–O_{ax}–N bond angle is the most important structural factor for the magnetic behavior of the nitroxide complexes of ruthenium(II,III) carboxylates, similarly to the nitroxide complexes of rhodium(II) carboxylates.[5c,h,8e] In the case of the ruthenium(II,III) nitroxide complexes, two coupling parameters, J_{M-R} and J_{R-R}, should be taken into consideration because the Ru(II,III) dimer has three unpaired electrons within the dimer core. This is one of the important points that are different from the rhodium(II) nitroxide complexes having no unpaired electron within the dimer core, in which J_{R-R} is only needed for the magnetic analysis, and has been investigated for its correlation with the axial bond angle Rh–O_{ax}–N(nitoxide).[8e] In Table 4, the J_{M-R} and J_{R-R} values and the axial

Table 4. Structural Parameters and J Values for the Axially O-Bonded Nitroxide Complexes of $[M_2(O_2CR)_4]^{0/+}$ Dimers (M = Ru and Rh)

Complex	M–O_{ax}/Å	M–O_{ax}–N/°	J_{M-R}/cm^{-1}	J_{R-R}/cm^{-1}	Ref.
$[Ru_2(O_2CCMe_3)_4(nitph)]_n(BF_4)_n$ (**1**)	2.264(8)	131.7(7)	0	—[a]	5c
	2.236(8)	147.5(7)	−100	0	
$[Ru_2(O_2CCMe_3)_4(nitme)_2]BF_4 \cdot 2CH_2Cl_2$ (**2**)	2.239(4)	123.7(4)	5	−40	This work
$[\{Ru_2(O_2CCMe_3)_4(nitme)_2\}\{Ru_2(O_2CCMe_3)_4(H_2O)_2\}]_n(BF_4)_{2n} \cdot 2nCH_2Cl_2$ (**4**)	2.269(8)	121.5(6)	20	−50	This work
$[\{Ru_2(O_2CCMe_3)_4(nitet)_2\}\{Ru_2(O_2CCMe_3)_4(H_2O)_2\}]_n(BF_4)_{2n} \cdot 2nCH_2Cl_2$ (**5**)	2.270(9)	122.5(7)	20	−47	This work
$[Ru_2(O_2CCMe_3)_4(nitph)(H_2O)]BF_4$ (**6**)	2.260(6)	137.7(5)	−45	—[b]	5h
$[Ru_2(O_2CCMe_3)_4(tempo)_2]$-$[Ru_2(O_2CCMe_3)_4(H_2O)_2](BF_4)_2$ (**7**)	2.184(3)	151.5(3)	−130	0	5a
$[Ru_2(O_2CCMe_3)_4(p\text{-nitpy})]_n(BF_4)_n$ (**8**)	2.286(7)	125.3(6)	20	—[b]	5d
$[Ru_2(O_2CCF_3)_4(tempo)_2]$ (**9**)	2.136(5)	158.2(3)	−263	0	9
$[Rh_2(O_2CCF_3)_4(tempo)_2]$ (**10**)	2.220(2)	138.0(1)	—[c]	−239	8c
$[Rh_2(O_2CC_3F_7)_4(tempo)_2]$ (**11**)	2.235(5)	134.2(4)	—[c]	−269	8c
$[Rh_2(O_2CCF_3)_4(nitph)_2]$ (**12**)	2.239(3)	122.7(3)	—[c]	−83.6	8e
$[Rh_2(O_2CCF_3)_4(nitme)]_n$ (**13**)	2.268(5)	118.3(4)	—[c]	−98.8	8e
	2.254(5)	121.3(4)			

a) One (147.5(7)°) of the two axial bond angles is not suited for operating the radical–radical interaction, resulting in no observation of the interaction between the radicals.[5c] b) One of the two axial sites of Ru(II,III) core is only coordinated by the N–O group of the radical.[5d,h] c) The Rh(II,II) dimer core is diamagnetic.

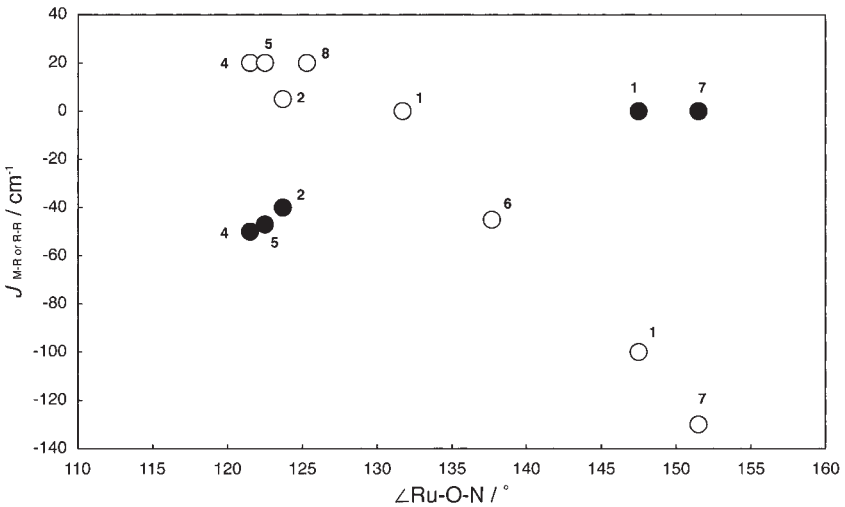

Fig. 11. Plots of the experimental J_{M-R} (○) and J_{R-R} (●) values versus Ru–O_{ax}–N bond angles. Numbers refer to the complexes listed in Table 4.

bond angles (M–O_{ax}–N) as well as the axial bond distances (M–O_{ax}) are summarized for the nitroxide complexes of $[M_2(O_2CR)_4]^{+/0}$ (M = Rh and Ru). The M–O_{ax}–N bond angles of Rh(II) complexes are located at 118–138°, of which the angles have been suggested to be suited for an antiferromagnetic interaction between the radicals through the σ* (or σ) orbital within the Rh(II) dimer core.[8] The axial bond angle value of the Ru(II,II) complex **9** is 158.2(3)°, which is unfavorable for the radical–radical interaction, but suited for the antiferromagnetic interaction between the Ru(II,II) core and the nitroxide radicals ($J_{M-R} = -263\,cm^{-1}$). The bond angles of the Ru(II,III) complexes are scattered in the range 122–152°. The J_{M-R} and J_{R-R} and Ru–O_{ax}–N angle values are plotted in Fig. 11. It can be seen that, with an increase in the angle ∠Ru–O–N, J_{M-R} and J_{R-R} are decreased and increased, respectively. When ∠Ru–O–N is around 120°, J_{M-R} is positive, whereas J_{R-R} is negative, as in the cases of the rhodium(II) nitroxide complexes, which seems to be interesting because the ferro- and antiferromagnetic interactions are both operative through the same M–O_{ax} bond. Positive J_{M-R} (5 and 20 cm^{-1}) and negative J_{R-R} (−40 to −50 cm^{-1}) values were observed for **2**, **4** and **5**, having the Ru–O_{ax}–N angles close to 120° (121.5(6)–123.7(4)°).

It is well known that the spin-coupling constant J is related to the overlap integral between the magnetic orbitals; the lager is the overlap, the more antiferromagnetic is the interaction.[19–21] An analysis based on the overlap integrals was applied to estimate the strength of the antiferromagnetic interaction between radicals through the Rh–Rh bond for Rh(II) dimers with radicals, where the magnetic orbitals mainly consist of the σ* (or σ) orbital of the dimeric core and the π* orbital of the radical.[8e] The overlap

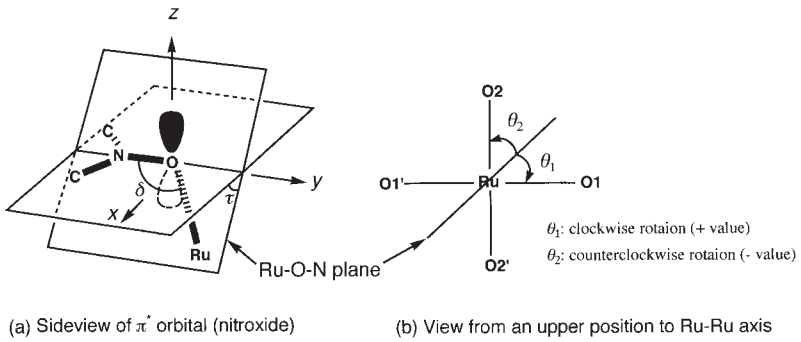

Scheme 2.

integral is proportional to the product of the coefficient associated with the π^*-electron spin population on the axially bound oxygen atom of the radical, and the angular part, which is expressed here by A_σ ($= (\sin\delta \sin\tau)^2$).[8e,22] In the case of nitroxide Ru(II,III) complexes, the σ^* (or σ) and π^* orbitals of Ru(II,III) core and π^* orbital of the radical should be taken into consideration as the magnetic orbitals.[5c,23] The J_{R-R} value (for the magnetic interaction between the radicals through the Ru–Ru bond) is related to A_σ as in the case of the rhodium(II) nitroxide complexes. In the case of J_{M-R} (for the magnetic interaction between the Ru(II,III) dimeric core and the radical), the magnitude is considered to be related to A_π ($= \sqrt{{A_{\pi 1}}^2 + {A_{\pi 2}}^2}$, where $A_{\pi t} = \sin\theta_t \cos\tau - \cos\theta_t \cos\delta \sin\tau$, $t = 1$ and 2);[24] $A_{\pi t}$ is an angular part based on the π^* (radical)–π^* (Ru(II,III) dimer) overlap, the inner product between the unit vectors corresponding to the orbitals, and can be obtained as described in Appendix. The parameters needed to calculate A_σ and A_π are defined in Scheme 2, assuming that the Ru, Ru′ and O (radical) atoms are collinear, and the Ru–O_{ax} distances are the same (~2.25 Å, except for the tempo complex **7** (2.136(5) Å)). The calculated A_σ and A_π values are given with the structural data for **1**, **2** and **4**–**8** in Table 5. Furthermore, in order to estimate the trends of the J_{M-R} and J_{R-R} values for the axial bond angle δ (∠Ru–O–N), the A_σ and A_π values were calculated while changing the angle ∠Ru–O–N; the other parameters (θ_1, θ_2, and τ) were fixed at 45°, −45°, and 75°, respectively, considering the structural data listed in Table 5. The result displayed in Fig. 12 shows that A_σ and A_π are decreased and increased, respectively, with increasing ∠Ru–O–N. The trend is consistent with that shown by the experimental results (Fig. 11) when taking into account that the larger overlap leads to a larger antiferromagnetic interaction. The A_σ and A_π values given in Table 5 are also consistent with the trend shown in Fig. 12, which implies that τ, θ_1, and θ_2 are not significant parameters affecting the trend by δ (∠Ru–O–N). Although J_{M-R} ($= -130\ \mathrm{cm}^{-1}$) of **7** might be rather small in absolute value when taking into account that the spin population of the oxygen of tempo is nearly twice as large as that of nitme,[8e] the results shown in Figs. 11 and 12 suggest that the axial bond angle, ∠Ru–O–N, should be the most important structural factor for the J_{R-R} and J_{M-R} values.

Table 5. Structural Parameters for the Ruthenium(II,III) Nitroxide Complexes

Complex	δ/°	τ/°	θ_1/°	θ_2/°	A_σ	A_π
1	131.7	81	46	−44.1	0.54	0.67
	147.5	38	84	−8	0.11	0.93
2	123.7	73.8	12	−76.9	0.64	0.60
4	121.5	76.8	16	−74.9	0.69	0.56
5	122.5	74.9	18	−72.3	0.66	0.58
6	137.7	69.6	41.2	−49.3	0.40	0.77
7	151.5	65	48	−42	0.19	0.90
8	125.3	86.5	25.5	−64.4	0.66	0.58

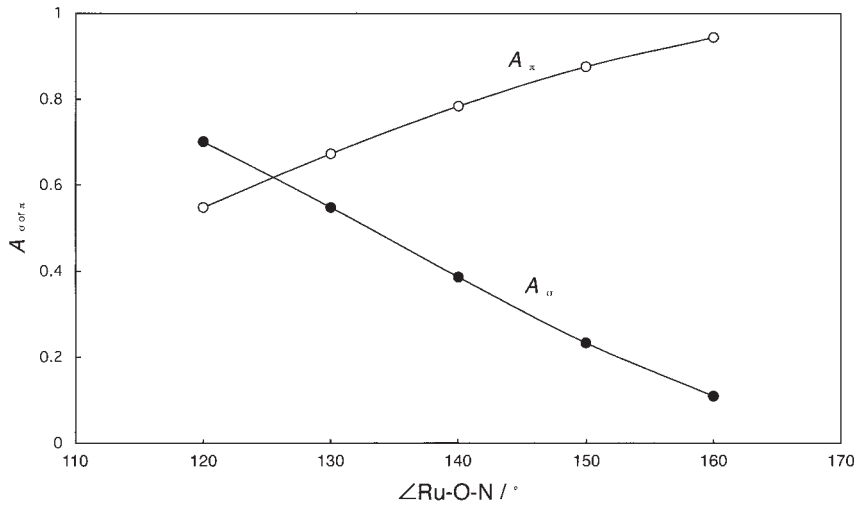

Fig. 12. Variations of the calculated A_π (○) and A_σ (●) values with Ru–O_{ax}–N bond angle δ.

Conclusions

The nitroxide dimer and chain complexes of ruthenium(II,III) pivalate dimers, $[Ru_2(O_2CCMe_3)_4(L)_2]BF_4$ and $[\{Ru_2(O_2CCMe_3)_4(L)_2\}\{Rh_2(O_2CCMe_3)_4(H_2O)_2\}]_n(BF_4)_{2n}$ (L = 2,4,4,5,5-pentamethyl-4,5-dihydro-1*H*-imidazol-1-oxyl-3-*N*-oxide (nitme) and 2-ethyl-4,4,5,5-tetramethyl-4,5-dihydro-1*H*-imidazol-1-oxyl-3-*N*-oxide (nitet)), were prepared depending on the Ru(II,III)–radical molar ratio employed for the reactions in CH_2Cl_2/hexane; the excess of the radical ligand to ruthenium(II,III) pivalate gave exclusively dimer complexes $[Ru_2(O_2CCMe_3)_4(L)_2]BF_4$, while the equimolar reaction produced chain complexes, $[\{Ru_2(O_2CCMe_3)_4(L)_2\}\{Rh_2(O_2CCMe_3)_4(H_2O)_2\}]_n(BF_4)_{2n}$. In the chain complexes, the Ru(II,III) dimer units are linked by hydrogen bonds between the axial water and the radical ligands. Because the hydrogen bond does not mediate any important magnetic interaction, the magnetic behaviors of the complexes could be interpreted as the sum of the magnetically independent two dimer units, $[Ru_2(O_2CCMe_3)_4(L)_2]^+$ and $[Ru_2(O_2CCMe_3)_4(H_2O)_2]^+$. Although the one-dimensional behaviors, e.g., ferrimagnetism,[13] were not observed for the present complexes of the ruthenium(II,III) pivalate and nitonyl nitroxide radicals, it was found that, in the obtained dimer and chain complexes, ferro- and antiferromagnetic interactions operate through the same axial Ru–O_{ax} bond, of which the situation could be reasonably interpreted by considering the overlaps between the σ^* (or σ) and π^* orbitals of the Ru(II,III) dimer core and π^* orbital of the radical; the Ru(II,III) dimer can offer two types of interactions using σ^* (or σ) and π^* orbitals within the dimer core between the axial radical ligands (estimated by J_{R-R}) and between the radical and the Ru(II,III) dimer core (estimated by J_{M-R}); the signs and magnitude of J_{R-R} and J_{M-R} are predominantly dependent on the axial Ru–O_{ax}–N bond angle. It was concluded that the bond angles around 120° gave ferro- and antiferromagnetic interactions ($J_{R-R} < 0$ cm^{-1} and $J_{M-R} > 0$ cm^{-1}).

Appendix

Angular Part $A_{\pi t}$. The π^* orbital of the nitorxide radical is depicted in Schemes 2 and 3. Two π^* orbitals of the Ru(II,III) core extend along the O1–O1′ and O2–O2′ axes, respectively, when being viewed from an upper position to the Ru–Ru axis. The oxygen atom of the N–O group is fixed at the origin (0, 0, 0) of the cartesian coordinate system, and the plane defined by C(NO)C (nitroxide) is situated on the *xy* plane, the *z* axis being perpendicular to the C(NO)C plane and parallel to the π^* (nitroxide) orbital. The unit vectors perpendicular to Ru–O–N plane and along O–M bond become

$$\boldsymbol{P} = (\sin\tau, 0, \cos\tau)$$

and

$$\boldsymbol{Q} = (\sin\delta\cos\tau, -\cos\delta, -\sin\delta\sin\tau), \quad \text{respectively.}$$

The unit vector $\boldsymbol{R}$ perpendicular to the vectors $\boldsymbol{P}$ and $\boldsymbol{Q}$ is obtained by their product:

$$\boldsymbol{R} = \boldsymbol{P} \times \boldsymbol{Q},$$

$$\boldsymbol{R} = (\cos\delta\cos\tau, \sin\delta, -\cos\delta\sin\tau).$$

When a π^* orbital of Ru(II,III) core is projected onto the plane made by O1, O1′, O2, and O2′ atoms, on which vectors $\boldsymbol{P}$ and $\boldsymbol{R}$ are situated, the unit vector $\boldsymbol{S}$ along the Ru–O1 or Ru–O2 direction can be described by vectors $\boldsymbol{P}$ and $\boldsymbol{R}$ using the parameter θ_t (see Scheme 3):

$$\boldsymbol{S} = (\sin\theta_t)\boldsymbol{P} + (\cos\theta_t)\boldsymbol{R}$$
$$= (\sin\theta_t\sin\tau + \cos\theta_t\cos\delta\cos\tau, \cos\theta_t\sin\delta, \sin\theta_t\cos\tau - \cos\theta_t\cos\delta\sin\tau).$$

The *z* component of vector $\boldsymbol{S}$ corresponds to the angular part, $A_{\pi t}$:

$$A_{\pi t} = \sin\theta_t\cos\tau - \cos\theta_t\cos\delta\sin\tau.$$

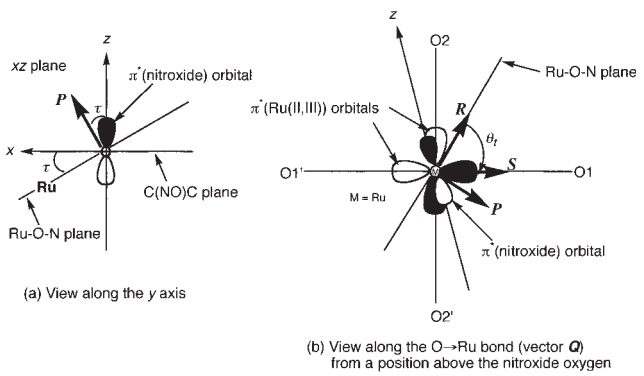

Scheme 3.

The present work was partially supported by Grants-in-Aid for Scientific Research No. 14540516 from the Ministry of Education, Culture, Sports, Science and Technology.

References

1 a) F. A. Cotton and R. A. Walton, "Multipule Bonds between Metal Atoms," 2nd ed, Oxford Univ. Press, New York (1993), pp. 399–430. b) M. A. S. Aquino, *Coord. Chem. Rev.*, **170**, 141 (1998).

2 a) J. G. Norman, Jr., G. E. Renzoni, and D. A. Case, *J. Am. Chem. Soc.*, **101**, 5256 (1979). b) V. M. Miskowski and H. B. Gray, *Inorg. Chem.*, **27**, 2501 (1988). c) P. Maldivi, A.-M. Giroud-Godquin, J.-C. Marchon, D. Guillon, and A. Skoulios, *Chem. Phys. Lett.*, **157**, 552 (1989). d) F. A. Cotton, V. M. Miskowski, and B. Zhong, *J. Am. Chem. Soc.*, **111**, 6177 (1989). e) G. Estiú, F. D. Cukiernik, P. Maldivi, and O. Poizat, *Inorg. Chem.*, **38**, 3030 (1999).

3 e.g., a) F. A. Cotton, Y. Kim, and T. Ren, *Inorg. Chem.*, **31**, 2723 (1992). b) D.-Q. Li, S. C. Huckett, T. Frankcom, M. T. Paffett, J. D. Farr, M. E. Hawley, S. Gottesfeld, J. D. Thompson, C. J. Burns, and B. I. Swanson, *ACS Symp. Ser.*, **449**, 33 (1992). c) K. R. Dunbar, *J. Cluster Sci.*, **5**, 125 (1994). d) F. D. Cukiernik, A.-M. Giroud-Godquin, P. Maldivi, and J.-C. Marchon, *Inorg. Chim. Acta*, **215**, 203 (1994). e) L. Bonnet, F. D. Cukiernik, P. Maldivi, A.-M. Giroud-Godquin, and J.-C. Marchon, *Chem. Mater.*, **6**, 31 (1994). f) E. J. Beck, K. D. Drysdale, L. K. Thompson, L. Li, C. A. Murphy, and M. A. S. Aquino, *Inorg. Chim. Acta*, **279**, 121 (1998). g) F. D. Cukiernik, D. Luneau, J.-C. Machon, and P. Maldivi, *Inorg. Chem.*, **37**, 3698 (1998). h) H. Miyasaka, C. S. Campos-Fernández, R. Clérac, and K. R. Dunbar, *Angew. Chem. Int. Ed.*, **39**, 3831 (2000). i) H. Miyasaka, R. Clérac, C. S. Campos-Fernández, and K. R. Dunbar, *J. Chem. Soc., Dalton Trans.*, **2001**, 858. j) H. Miyasaka, C. Kachi-Terajima, T. Ishii, and M. Yamashita, *J. Chem. Soc., Dalton Trans.*, **2001**, 1929. k) H. Miyasaka, R. Clérac, C. S. Campos-Fernández, and K. R. Dunbar, *Inorg. Chem.*, **40**, 1663 (2001); J.-L.

Zuo, E. Herdtweck, and F. E. Kühn, *J. Chem. Soc., Dalton Trans.*, **2002**, 1244. l) Y. Liao, W. W. Shum, and J. S. Miller, *J. Am. Chem. Soc.*, **124**, 9336 (2002).

4 a) M. Handa, D. Yoshioka, Y. Sayama, K. Shiomi, M. Mikuriya, I. Hiromitsu, and K. Kasuga, *Chem. Lett.*, **1999**, 1033. b) D. Yoshioka, M. Handa, H. Azuma, M. Mikuriya, I. Hiromitsu, and K. Kasuga, *Mol. Cryst. Liq. Cryst.*, **342**, 133 (2000). c) M. Handa, D. Yoshioka, I. Hiromitsu, and K. Kasuga, *Mol. Cryst. Liq. Cryst.*, **376**, 257 (2002). d) D. Yoshioka, M. Mikuriya, and M. Handa, *Chem. Lett.*, **2002**, 1044.

5 a) M. Handa, Y. Sayama, M. Mikuriya, R. Nukada, I. Hiromitsu, and K. Kasuga, *Bull. Chem. Soc. Jpn.*, **68**, 1647 (1995). b) M. Handa, Y. Sayama, M. Mikuriya, R. Nukada, I. Hiromitsu, and K. Kasuga, *Chem. Lett.*, **1996**, 201. c) M. Handa, Y. Sayama, M. Mikuriya, R. Nukada, I. Hiromitsu, and K. Kasuga, *Bull. Chem. Soc. Jpn.*, **71**, 119 (1998). d) Y. Sayama, M. Handa, M. Mikuriya, I, Hiromitsu, and K. Kasuga, *Chem. Lett.*, **1998**, 777. e) Y. Sayama, M. Handa, M. Mikuriya, I. Hiromitsu, and K. Kasuga, *Chem. Lett.*, **1999**, 453. f) Y. Sayama, M. Handa, M. Mikuriya, R. Nukada, I. Hiromitsu, and K. Kasuga, in ''Coordination Chemistry at the Turn of the Century,'' ed by G. Ondrejovic and A. Sirota, Slovak. Tech. Univ. Press, Bratislava (1999), pp. 447–452. g) Y. Sayama, M. Handa, M. Mikuriya, I. Hiromitsu, and K. Kasuga, *Bull. Chem. Soc. Jpn.*, **73**, 2499 (2000). h) Y. Sayama, M. Handa, M. Mikuriya, I. Hiromitsu, and K. Kasuga, *Bull. Chem. Soc. Jpn.*, **74**, 2129 (2001).

6 e.g., a) H. O. Stumpf, L. Ouahab, Y. Pei, P. Bergerat, and O. Kahn, *J. Am. Chem. Soc.*, **116**, 3866 (1994). b) K. Inoue and H. Iwamura, *Angew. Chem. Int. Ed. Engl.*, **34**, 927 (1995). c) S. Karasawa, Y. Sano, T. Akita, N. Koga, T. Itoh, H. Iwamura, P. Rabu, and M. Drillon, *J. Am. Chem. Soc.*, **120**, 10080 (1998). d) V. N. Ikorskii, V. I. Ovcharenko, Y. G. Shvedenkov, G. V. Romanenko, S. V. Fokin, and R. Z. Sagdeev, *Inorg. Chem.*, **37**, 4360 (1998). e) T. Yoshida, T. Suzuki, K. Kanamori, and S. Kaizaki, *Inorg. Chem.*, **38**, 1059 (1999). f) K. E. Vostrikova, D. Luneau, W. Wernsdorfer, P. Rey, and M. Verdaguer, *J. Am. Chem. Soc.*, **122**, 718 (2000). g) D. A. Shultz, S. H. Bondnar, K. E. Vostrikova, and J. W. Kampf, *Inorg. Chem.*, **39**, 6091 (2000). h) H. Oshio and T. Ito, *Coord. Chem. Rev.*, **198**, 329 (2000). i) A. Caneschi, D. Gatteschi, N. Lalioti, C. Sangregorio, R. Sessoli, G. Venturi, A. Vindigni, A. Rettori, M. G. Pini, and M. A. Novak, *Angew. Chem. Int. Ed.*, **40**, 1760 (2001). j) C. Stroh, P. Turek, R. Rabu, and R. Ziessel, *Inorg. Chem.*, **40**, 5334 (2001). k) H. Oshio, M. Yamamoto, T. Ito, H. Kawauchi, N. Koga, T. Ikoma, and S. Tero-Kubota, *Inorg. Chem.*, **40**, 5518 (2001). l) T. M. Barclay, R. G. Hicks, M. T. Lemaire, and L. K. Thompson, *Inorg. Chem.*, **40**, 6521 (2001). m) U. Schatzschneider, T. Weyhermüller, and E. Rentschler, *Eur. J. Inorg. Chem.*, **2001**, 2569. n) J. Omata, T. Ishida, D. Hashizame, F. Iwasaki, and T. Nogami, *Inorg. Chem.*, **40**, 3954 (2001). o) D. Zhang, L. Ding, W. Xu, H. Hu, D. Zhu, Y. Huang, and D. Fang, *Chem. Commun.*, **2002**, 44. p) L. M. Field, P. M. Lahti, and F. Palacio, *Chem. Commun.*, **2002**, 636. q) M. Minguet, D. Luneau, E. Lhotel, V. Villar, C. Paulsen, D. B. Amabilino, and J. Veciana, *Angew. Chem. Int. Ed.*, **41**, 586 (2002). r) M. Mikuriya, H. Azuma, J. Sun, D. Yoshioka, and M. Handa, *Chem. Lett.*, **2002**, 608. s) L. Li, D. Liao, Z. Jiang, and S. Yan, *J. Chem. Soc., Dalton Trans.*, **2002**, 1350. t) C. Lescop, E. Belorizky, D. Luneau, and P. Rey, *Inorg. Chem.*, **41**, 3375 (2002). u) M. Fettouchi, B. E. Ali, A. M. El-Ghanam, S. Golhen. L. Ouahab, N. Daro, and J.-P. Sutter, *Inorg. Chem.*, **41**, 3705 (2002). v) C. Benelli and D. Gatteschi, *Chem. Rev.*, **102**, 2369 (2002).

7 a) A. Caneschi, D. Gatteschi, and R. Sessoli, *Acc. Chem. Res.*, **22**, 392 (1989). b) A. Caneschi, D. Gatteschi, and P. Rey, *Prog. Inorg. Chem.*, **39**, 331 (1991).

8 a) R. M. Richman, T. C. Kuechler, S. P. Tanner, and R. S. Drago, *J. Am. Chem. Soc.*, **99**, 1055 (1977). b) T.-Y. Dong, D. N. Hendrickson, T. R. Felthouse, and H.-S. Shieh, *J. Am. Chem. Soc.*, **106**, 5373 (1984). c) T. R. Felthouse, T.-Y. Dong, D. N. Hendrickson, H.-S. Shieh, and, M. R. Thompson, *J. Am. Chem. Soc.*, **108**, 8201 (1986). d) A. Cogne, A. Grand, P. Rey, and R. Subra, *J. Am. Chem. Soc.*, **109**, 7929 (1987). e) A. Cogne, A. Grand, P. Rey, and R. Subra, *J. Am. Chem. Soc.*, **111**, 3230 (1989).

9 A. Cogne, E. Belorizky, J. Laugier, and P. Rey, *Inorg. Chem.*, **33**, 3364 (1994).

10 a) Y.-H. Chung, H.-H. Wei, G.-H. Lee, and Y. Wang, *Inorg. Chim. Acta*, **293**, 30 (1999). b) Y.-H. Chung and H.-H. Wei, *Inorg. Chem. Commun.*, **2**, 269 (1999). c) M. Mikuriya, H. Azuma, R. Nukada, Y. Sayama, K. Tanaka, J.-W. Lim, and M. Handa, *Bull. Chem. Soc. Jpn.*, **73**, 2493 (2000). d) I. Dasna, S. Golhen, L. Ouahab, O. Peña, N. Daro, and J.-P. Sutter, *New J. Chem.*, **24**, 903 (2000).

11 M. C. Barral, R. Jiménez-Aparicio, J. L. Priego, E. C. Royer, E. Gutiénez-Puebla, and C. Ruiz-Valero, *Polyhedron*, **11**, 2209 (1992).

12 a) E. F. Ullman, L. Gall, and J. H. Osiecki, *J. Org. Chem.*, **35**, 3623 (1970). b) M. S. Davis, K. Morokuma, and R. W. Kreilick, *J. Am. Chem. Soc.*, **94**, 5588 (1972).

13 O. Kahn, ''Molecular Magnetism,'' VCH Publishers Inc. (1993).

14 C. K. Fair, ''MolEN Structure Determination System,'' Delft Instrument, Delft (1990).

15 a) W. Wong and S. F. Watkins, *J. Chem. Soc., Chem. Commun.*, **1973**, 888. b) A. Grand, P. Rey, R. Subra, V. Barone, and C. Minichino, *J. Phys. Chem.*, **95**, 9238 (1991). c) F. L. Panthou, D. Luneau, J. Laugier, and P. Rey, *J. Am. Chem. Soc.*, **115**, 9095 (1993). d) A. Zheludev, V. Barone, M. Bonnet, B. Delley, A. Grand, E. Ressouche, P. Rey, R. Subra, and J. Schweizer, *J. Am. Chem. Soc.*, **116**, 2019 (1994).

16 A. Caneshchi, L. Laugier, and P. Rey, *J. Chem. Soc., Perkin Trans. 1*, **1987**, 1077.

17 F. A. Cotton and T. R. Felthouse, *Inorg. Chem.*, **21**, 2667 (1982).

18 a) J. Telser and R. S. Drago, *Inorg. Chem.*, **23**, 3114 (1984). b) J. Telser, V. M. Miskowski, R. S. Drago, and N. M. Wong, *Inorg. Chem.*, **24**, 4765 (1985). c) M. C. Barral, R. Jiménez-Aparicio, D. Pérez-Quintanilla, J. L. Priego, E. C. Royer, M. R. Torres, and F. A. Urbanos, *Inorg. Chem.*, **39**, 65 (2000). d) R. Jiménez-Aparicio, F. A. Urbanos, and J. M. Arrieta, *Inorg. Chem.*, **40**, 613 (2001).

19 P. J. Hay, J. C. Thibeault, and R. Hoffman, *J. Am. Chem. Soc.*, **97**, 4884 (1975).

20 O. Kahn, *Inorg. Chim. Acta*, **62**, 3 (1982).

21 a) A. Caneschi, D. Gatteschi, A. Grand, J. Laugier, L. Pardi, and P. Rey, *Inorg. Chem.*, **27**, 1031 (1988). b) D. Luneau, P. Rey, J. Laugier, P. Fries, A. Caneschi, D. Gatteschi, and R. Sessoli, *J. Am. Chem. Soc.*, **113**, 1245 (1991).

22 In Ref. 8e, the author compared the obtained J_{R-R} values based on $S^2 \propto (\sin\delta \sin\tau)^2$, which should be $(\sin\delta \sin\tau)^4$ according to their explanation on the overlap integral, $S\ (\propto \langle\sigma(\mathrm{Rh(II)})|\pi^*(\mathrm{nitroxide})\rangle^2 = (\sin\delta \sin\tau)^2)$ in the reference.

23 The δ^* orbital of Ru(II,III) dimer core is not taken into consideration because the orbital is not spread into the space suitable for the overlap with the π^* orbital of the nitroxide radical.

24 The exchange integral J can be divided into two parts: $J = J_F + J_{AF}$, where J_F is the term for the ferromagnetic contribution and J_{AF} the term for the antiferromagnetic contribution (see Chapter 9 in Ref. 13). The term J_{AF} is the negative component of J and roughly proportional to $-S^2$, where S is the overlap integral

between magnetic orbitals. It is difficult to correlate J with the overlap integrals between the magnetic orbitals where there are more than two unpaired electrons in the two magnetic centers; two π^* (Ru(II,III)) and one π^* (nitroxide) unpaired electrons reside in the magnetic orbitals. However, it seems reasonable to suppose that the antiferromagnetic contribution is related to summation of $-S_i^2$ ($\Sigma - S_i^2$; $S_i \propto A_i$) even in the present case. Because summation of A_i^2 can be regarded as magnetically more significant than that of A_i, we here defined A_π by $\sqrt{A_{\pi 1}^2 + A_{\pi 2}^2}$ as the angular part of the overlap integral related to J_{M-R} in order to estimate the trend of J_{M-R} vs δ.